

FULL PAPER

Anisotropic atomic layer etching of W using fluorine radicals/oxygen ion beam

Doo San Kim¹ | Ju Eun Kim¹ | Won Oh Lee¹ | Jin Woo Park¹ | You Jung Gill¹ |
Byeong Hwa Jeong^{1,2} | Geun Young Yeom^{1,3} 

¹School of Advanced Materials Science and Engineering, Sungkyunkwan University, Suwon, Republic of Korea

²Korea Institute for Super Materials, ULVAC KOREA, Pyeongtaek, Republic of Korea

³SKKU Advanced Institute of Nano Technology (SAINT), Sungkyunkwan University, Suwon, Republic of Korea

Correspondence

Geun Young Yeom, School of Advanced Materials Science and Engineering, Sungkyunkwan University, Suwon 16419, Republic of Korea.

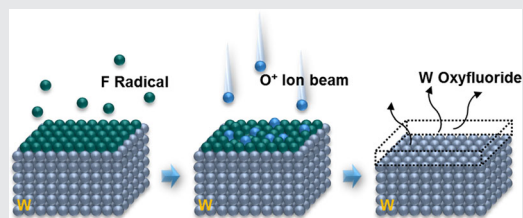
Email: gyeom@skku.edu

Funding information

the Korean government (MSIT), Grant/Award Number: 2018R1A2A3074950; Ministry of Education, Science, and Technology, Grant/Award Number: 2016M3A7B4910429

Abstract

Atomic layer etching (ALE) has advantages such as precise thickness control, high etch selectivity, and no-increase in surface roughness which can be applied to sub 10 nm semiconductor device fabrication. In this study, anisotropic ALE of tungsten (W), which is used as an interconnect layer and gate material of semiconductor devices, was investigated by sequentially exposing to F radicals by NF_3 plasma to form a WF_y layer and following exposure to an oxygen ion beam to remove the WF_y layer by forming volatile WO_xF_y at room temperature. A wide ALE window of F radical adsorption time of (≥ 10 s/cycle) and O_x^+ ion desorption time of ($10 \leq t \leq 50$ s/cycle at +44–51 eV of O_x^+ ion energy) could be identified, and at the ALE conditions, a precise etch rate of $\sim 2.6 \text{ \AA/cycle}$ was obtained while increasing the W etch depth linearly with increasing the number of etch cycles. At the optimized W ALE conditions, the W surface roughness after the W ALE was similar to the as-received W and the etch selectivity over SiO_2 was close to infinite. However, after the W ALE, $\sim 10\%$ F diffused into W was observed on the etched W surface, and which could be removed by a following process.



KEYWORDS

atomic layer etching (ALE), ion beam, NF_3 (nitrogen trifluoride), O_2 (oxygen), W (tungsten), XPS (X-ray photoelectron spectroscopy)

1 | INTRODUCTION

Recently, atomic layer etching (ALE) technology has attracted much attention due to miniaturization and high integration of semiconductor devices.^[1,2] This ALE technology can process semiconductors more precisely than

conventional reactive ion etching (RIE) and has advantages such as high etch selectivity, low surface damage, etc.^[3–5] In general, the ALE studies using plasmas have been investigated by adsorbing reactive gases such as radicals or reactive molecules on the surface for the modification of the surface by chemisorption, and then by removing the

modified surface layer only by using energetic ions. Using these techniques, a precise etch depth/cycle of various semiconductor related materials such as Si, III-V compounds, metals, and 2D materials has been achieved.^[6–11] As the plasma sources for radical adsorption, inductively coupled plasma (ICP) and capacitively coupled plasma (CCP) were mainly used^[12,13] while, as the desorption sources, an ion/neutral beam^[14,15] or conventional radio frequency (RF) biasing was used for anisotropic ALE technology. Recently, for the fabrication of nanoscale devices, in addition to the anisotropic ALE, isotropic ALE or also known as thermal ALE, where, materials are etched the same in all direction isotropically, is actively investigated. The thermal ALE uses an elevated temperature similar to atomic layer deposition (ALD) and, for the thermal ALE, a reactive molecule is chemisorbed on the surface to form a compound, and then the surface compound is removed by converting into a volatile compound with a second reactive molecule.^[16]

For semiconductor device fabrication, various metals such as aluminum (Al), copper (Cu), tungsten (W), titanium (Ti), cobalt (Co), molybdenum (Mo), etc have been investigated and applied for interconnecting devices. Among these metals, due to the very high conductivity (the highest next to Ag), Cu is currently used most commonly for metallization. However, for the critical dimension lower than tens of nanometer, it is reported that the resistivity of Cu is increased sharply due to the size effect related to the long electron mean free path (EMFP) of 39 nm^[17–23] in addition to the decreased reliability of Cu as the device operating temperatures and current densities are increased.^[24,25] As one of possible replacements of Cu, W, which is widely used as an interconnect layer, a diffusion barrier of semiconductor integrated circuits, a gate material for 3D NAND flash memory, etc^[26,27] is investigated for the next generation interconnection material because of the smaller EMFP of 19 nm and a high melting point (3,695 K compared with Cu of 1,357 K).^[18,19,24,28,29] Since W has a smaller EMFP than Cu, it is expected to reduce the size effect of surface scattering and grain boundary scattering as it goes to nanometer dimension.^[19,30]

For the application of W to next generation device interconnection, ALE technology of W is known to be required.^[31,32] For the W ALE method, a W thermal ALE obtained through an oxidation-conversion-fluorination etch mechanism, which is a three step ALE composed of oxidation using O₃, the conversion to a volatile oxychloride compound using BCl₃, and the final removal of the surface residue compound by fluorination by HF, is reported.^[33] In addition, a thermal ALE of W using sequential exposure to O₂ (or O₃) and WF₆, where, W is oxidized using O₂ or O₃ to form WO₃(s), and the WO₃ is

removed by forming volatile WO₂F₂(g) by the reaction with HF has been investigated.^[34] Even though, self-limited precise etching of W with the rates of a few Å/cycle could be obtained with the ALE methods investigated until now, all of these methods are isotropic W ALE methods and an anisotropic W ALE method which can form anisotropic etch profiles of W has not been investigated yet.

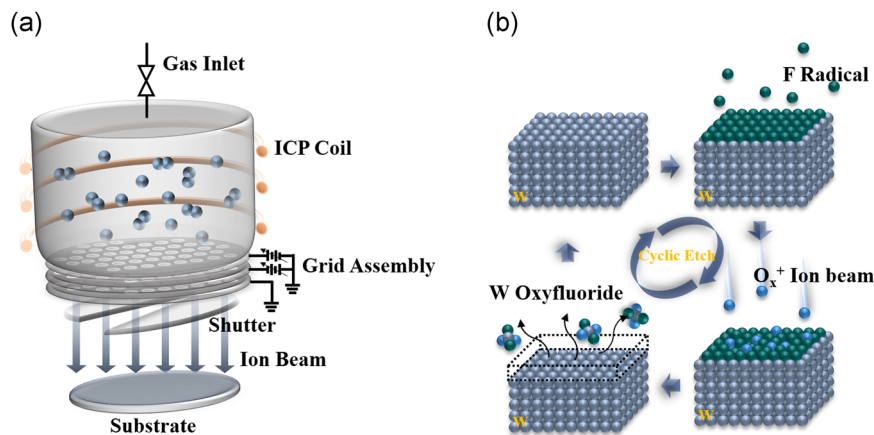
In this study, a possibility of anisotropic W ALE was investigated using NF₃ radicals and oxygen ion beam using an ion beam technology at room temperature for anisotropic and precise etching. In the adsorption step, the W surface was fluorinated using NF₃ radicals and then, in the desorption step, an oxygen ion beam was irradiated to form a volatile tungsten oxyfluoride (WO_xF_y) compound. The ALE window for the adsorption and desorption conditions was investigated and the W ALE mechanism was studied by analyzing the surface roughness, surface composition, and chemical binding states of W during the adsorption step and desorption step.

2 | EXPERIMENTAL

The W ALE system used in the experiment is shown in Figure 1(a). The W ALE system was consisted of a vacuum chamber with a 6-inch diameter ion beam source (a cylindrical inductively coupled plasma [ICP] source and a three graphite grid assembly) attached on the top of the chamber, a shutter below the ion beam source, and a substrate holder located 12 cm below the ion beam grids. The gases were injected to the top of the ion beam source and 13.56 MHz radio-frequency (RF) was applied to the ICP source. For the three-grid assembly, +DC voltage was applied to the first grid (acceleration grid) located close to the ICP source for the control of the energy of the ion beam, –DC voltage to the second grid (the extraction grid) for the control of the ion beam flux, and the third grid (ground grid) close to the substrate holder was grounded.

The anisotropic W ALE concept is shown in Figure 1(b). The anisotropic ALE consists of two sequential steps; (a) the adsorption step, where the surface is chemically modified by adsorbing the reactive gas to the material to be etched, and (b) the desorption step, where the modified surface layer is removed by energetic ion bombardment, and for a cyclic etch process, each step is repeated alternatively while purging the gases between two steps. For the W ALE, ~40 nm thick W thin film deposited on SiO₂ substrates using DC sputtering and patterned with a photoresist by a photolithographic process was used as the etch sample. During the

FIGURE 1 (a) Schematic diagram of an ICP ion beam source with a three-grid assembly used for anisotropic W ALE. (b) The concept of W ALE cycles by F radicals from a NF_3 plasma and an O_x^+ ion beam. ICP, inductively coupled plasma; W ALE, tungsten atomic layer etching



adsorption step, NF_3 gas was decomposed by the plasma and dissociated fluorine radicals were adsorbed on the W surface. For the NF_3 radical adsorption, 2 mTorr NF_3 was maintained at the vacuum chamber, and 300 W of RF power was applied to the ICP source while no voltages are applied to the grids and with the shield-on to prevent possible ion bombardment on the W surface from the ion source to the substrate during the adsorption step. The adsorption time was varied from 0 to 30 s. During the desorption step, oxygen ion (O_x^+) beam was extracted by forming O_2 plasma and to remove W by forming volatile tungsten oxyfluorides. For the oxygen ion beam, 1 mTorr O_2 was maintained at the vacuum chamber and 300 W of RF power was applied to the ICP source while applying +30–+100 V to the first grid and –100 V to the second grid. The desorption time was varied from 0 to 100 s. The substrate temperature was maintained at room temperature (RT) during the ALE process.

After the W ALE process, the W etch depth was measured by a surface profilometer (Tencor Instrument, Alpha step 500) after 100 cycles of ALE for the evaluation of the etched W thickness per cycle. The distribution of oxygen ion energy according to the first grid voltage for the analysis of the oxygen ion beam energy used in the desorption step was measured by a home-made retarding grid ion energy analyzer with a current meter (Keithley 2400) and a voltage meter (Hewlett Packard 34401A) installed at the sample location. Atomic force microscope (AFM; Bruker Innova) measurement was performed to investigate the change in root mean square (RMS) surface roughness during the W ALE processes. The surface compositions of W after the W ALE processes were analyzed using X-ray photoelectron spectroscopy (XPS; Thermo VG, MultiLab 2000, Mg $K\alpha$ source) to investigate the amount of fluorine adsorption on W during the adsorption step and the removal of fluorine by the oxygen ion during the desorption step.

3 | RESULTS & DISCUSSION

For the W ALE, as the first step, the F adsorption characteristics were investigated by observing the fluorine coverage on the W surface during the adsorption step. For the F radical adsorption on the W surface, 300 W of RF power was applied to the ICP source at 2 mTorr NF_3 in the processing chamber while no voltages are applied to the grids. The fluorine coverage on the W surface was observed using XPS after the exposure for 0 to 100 s at the adsorption condition. Figure 2(a) shows the changes in atomic percentages of W, F, and O on W surface measured by XPS with increasing F radical exposure time. The increase of F radical exposure time initially increased the fluorine percentage on the W surface until 10 s exposure by showing 0%, 34.2%, and 49.1% for 0, 5, and 10 s of exposure time, respectively. However, the further increase of exposure time to 20 and 30 s saturated the fluorine percentage by showing 50.3% and 50.1%, respectively. When the fluorine radical exposure time was further increased to 100 s, still similar fluorine percentage of 51.9% was observed. In the case of W and O (possibly due to the surface oxidation of as-received W), their atomic percentages were decreased with the F radical exposure time and saturated when the F radical exposure time was also higher than 10 s. Therefore, for the saturated coverage of fluorine on the W surface, the F radical exposure time equal to and higher than 10 s was required. During the F radical exposure at RT, no etching of W was observed (shown in Figure 3).

As the second step, to investigate the desorption condition with an oxygen ion beam, W was exposed to oxygen ion beams with different energies and the effect of oxygen ion beam on the formation of WO_x (because W is more easily oxidized by an oxygen ion beam rather than etching) was investigated without exposing the W on F radicals. For the oxygen ion beam, 300 W of RF power was applied to the ICP source at 1 mTorr of O_2 while

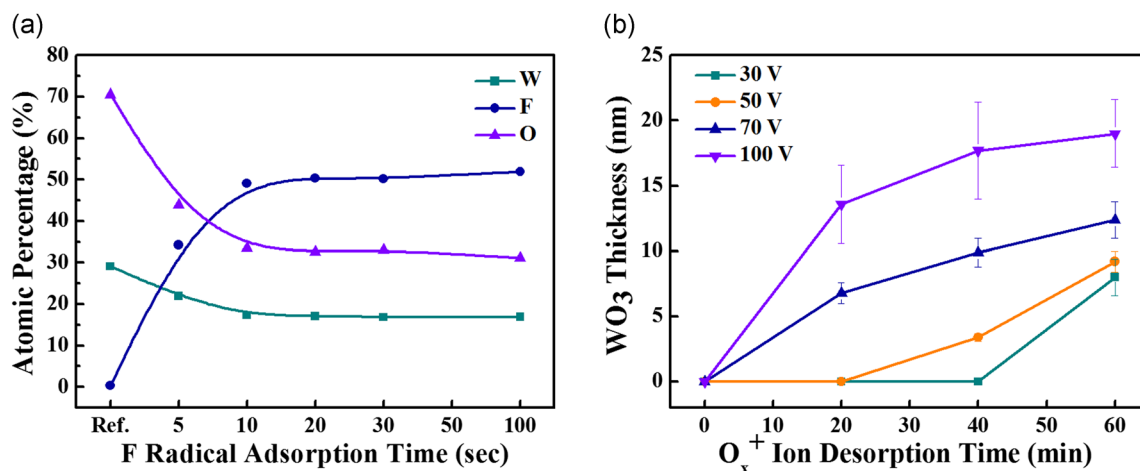


FIGURE 2 (a) Changes in atomic percentages of W, F, and O on W surface measured by XPS with increasing F radical exposure time. (b) Changes in WO_x thickness on the W surface measured by a surface profilometer with increasing first grid voltage from +30 to +100 V and O_x⁺ ion exposure time from 0 to 60 s. XPS, X-ray photoelectron spectroscopy

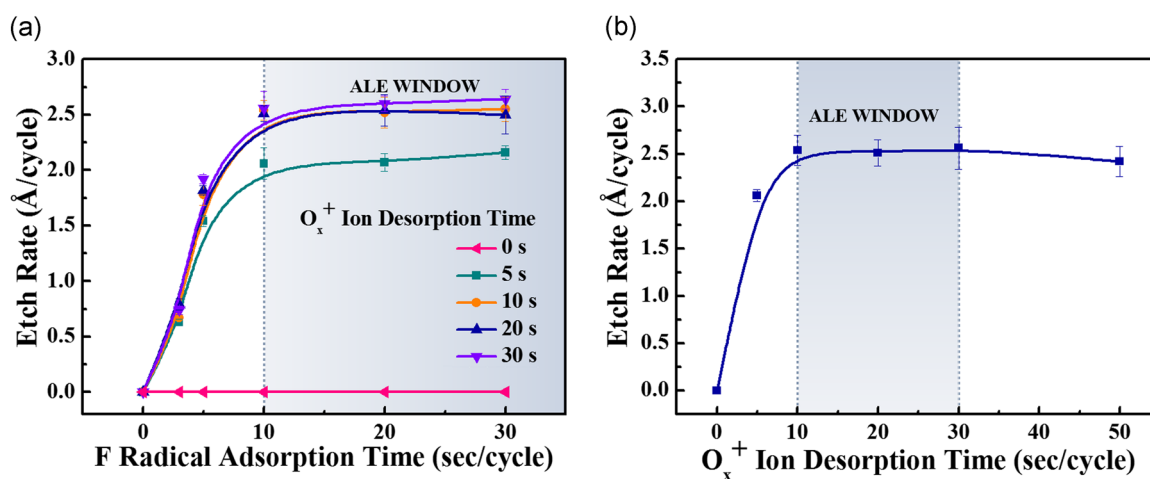


FIGURE 3 (a) Variation of W etch rate (depth/cycle) measured while varying the F radical adsorption time and O_x⁺ ion exposure time. To observe the saturated etch depth/cycle, the F radical adsorption time was varied from 0 to 30 s and the desorption time was varied from 0 to 30 s. The etch depth/cycle was measured after running 100 cycles. (b) Etch rate of W measured as a function of O_x⁺ ion desorption time/cycle while keeping the F radical adsorption time/cycle at 10 s/cycle

applying +30–+100 V to the first grid, –100 V to the second grid, and 0 V (grounded) to the third grid. The formation of WO_x was estimated by the increased W thickness after the oxygen ion beam exposure using a surface profilometer because, during the oxygen exposure, the thickness of W is increased by the formation of WO_x.^[33] (In fact, because it is difficult to measure the thickness of a self-limiting oxidation step of a few angstroms with a profilometer, the oxidation time was increased until the oxide thickness can be measured by the profilometer and the data were extrapolated to the lower oxidation time.) Figure 2(b) shows the changes in WO_x thickness on the W surface measured by the surface profilometer with increasing first grid voltage from +30 to +100 V and O_x⁺ ion exposure time from 0 to 60 s. The

first grid voltage is directly related to the oxygen ion energy from the ion source and the ion energy distributions measured by a retarding grid ion energy analyzer for the different first grid voltages are shown in Figure S1. As shown in Figure 2(b), when the first grid voltage was +30 V, no noticeable WO_x was observed on the W surface until 40 min of exposure time but noticeable WO_x formation of ~7 nm was observed when the exposure time was increased to 60 s. When the first grid voltage was increased to +50 V, the exposure time without WO_x formation was decreased to 20 min and the further increase of first grid voltage to +70 and +100 V, decreased the WO_x formation time <20 min in addition to thicker WO_x on the W surface. As the O_x⁺ ion energy for the desorption, no noticeable WO_x formation during

the desorption step is required, therefore, +30 V of first grid voltage (44–51 eV) was used as the desorption energy condition. When the formation of WO_x was further investigated during the ALE cycles just exposing to the oxygen ion beam (+30 V of first grid voltage) during the desorption step without adsorbing F radicals during the adsorption step, as shown in Figure S2, no WO_x formation was observed when the W was exposed equal to and <30 s/cycle.

Finally, using the adsorption conditions with F radicals (300 W of RF power to the ICP source, 2 mTorr NF_3 , and the adsorption time ≥ 10 s/cycle) and the desorption condition of the O_x^+ ion beam (300 W of RF power to the ICP source, 1 mTorr of O_2 , +30 V to the first grid, -100 V to the second grid, 0 V (grounded) to the third grid, and the desorption time ≤ 30 s/cycle), W was etched and the variation of etch depth/cycle was measured while varying the F radical adsorption time and O_x^+ ion desorption time, and the results are shown in Figure 3(a). To observe the saturated etch depth/cycle, the F radical adsorption time was varied from 0 to 30 s and the desorption time was also varied from 0 to 30 s. The etch depth/cycle was estimated after running 100 cycles. When W was exposed to F radicals up to 30 s/cycle without exposing to O_x^+ ion during the desorption step (that is, the desorption time = 0 s), no etching of W was observed indicating F radical adsorption on the W surface without spontaneous etching of W. As the F radical adsorbed W was exposed to O_x^+ ions, W was etched and, the etch depth/cycle was increased with the increase of F radical adsorption time and was saturated at ~ 10 s/cycle for the O_x^+ ion desorption time from 5 to 30 s/cycle. The saturation of W etch rate for the F radical adsorption time of ≥ 10 s/cycle regardless of O_x^+ ion desorption time indicates the full coverage of F radical on the W surface as shown in Figure 2(a) by forming WF_y .

The saturated etch rate was also increased with the O_x^+ ion desorption time/cycle during the desorption step by showing the saturated etch rate ~ 2.0 Å/cycle for 5 s and ~ 2.6 Å/cycle for the desorption time higher than 10 s/cycle when the F radical adsorption time is ≥ 10 s/cycle as shown in Figure 3(a). Figure 3(b) also shows the etch rate of W measured as a function of O_x^+ ion desorption time/cycle while keeping the F radical adsorption time/cycle at 10 s/cycle. The etch rate was saturated when the O_x^+ ion desorption time/cycle was higher than 10 s/cycle up to 50 s/cycle indicating the removal of the all of the WF_y by forming volatile WO_xF_y compounds.^[34] For the O_x^+ ion desorption time/cycle higher than 50 s/cycle, the further increase of W etch rate was observed possibly due to the formation of WO_x on the W surface as shown in Figure 2(b) or Figure S2 during the extended exposure to O_x^+ ions after the complete removal of WF_y on the surface by forming WO_xF_y (Figure S3). Therefore, the optimum O_x^+ ion desorption time/cycle for the saturated W etch rate was 10–50 s/cycle.

Using optimized adsorption/desorption conditions with F radicals (10 s/cycle) and O_x^+ ion beam (+30 V of first grid voltage, 10 s/cycle), the W etch depth and etch rate were investigated for 20–120 etch cycles and the result is shown in Figure 4(a). As shown in the figure, the etch depth was linearly increased with the increase of etch cycles, and the etch rate was remaining almost constant at ~ 2.6 Å/cycle. To investigate the etch selectivity of W with other materials, the etch rates for other materials such as SiO_2 and Si_3N_4 were also investigated with the optimized W ALE conditions and the result is shown in Figure 4(b). As shown, the etch rate about ~ 3 times higher than W etch rate was observed for Si_3N_4 while no etching was observed for SiO_2 possibly due to

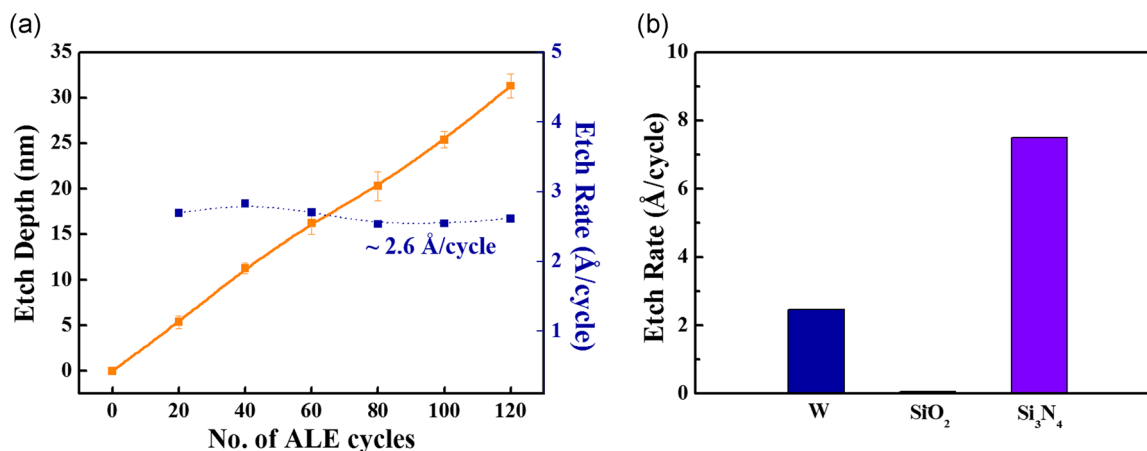


FIGURE 4 (a) W etch depth and etch rate at the optimized adsorption/desorption conditions with F radicals (10 s/cycle) and O_x^+ ion beam (+30 V of first grid voltage, 10 s/cycle) for 20–120 etch cycles. (b) Etch rates of SiO_2 and Si_3N_4 including W at the optimized W ALE condition showing the infinite etch selectivity over SiO_2 . W ALE, tungsten atomic layer etching

the differences in the bonding energies of Si-N (335 kJ/mol) and Si-O (444 kJ/mol).

The change of surface roughness during one ALE cycle was measured by AFM on $2.5\ \mu\text{m} \times 2.5\ \mu\text{m}$ W samples with the optimized W ALE conditions in Figure 4 and the results are shown in Figure 5. The RMS surface roughness for the as-received reference W was ~ 0.9 nm and, after the adsorption of F radicals for 10 s, the roughness was remaining at ~ 0.91 nm, therefore, no change of surface roughness was observed by the F radical adsorption on W. After the F radical adsorption, when the F-adsorbed W was desorbed by O_x^+ ions for 3 s and 5 s, the surface roughness was increased to 1.21 and 1.29 nm, respectively, due to the partial removal of WF_y by O_x^+ ions on the F-adsorbed W surface. However, when the desorption time was further increased to 10 s, the surface roughness was decreased to ~ 0.95 nm which is close to the as-received W. And the surface roughness was remaining similar at ~ 0.95 nm until the desorption time was increased to 30 s possibly due to the complete removal of the WF_y layer formed on the W surface during the F radical adsorption step for the desorption time ≥ 10 s. The AFM images for the conditions in Figure 5(a) are shown in Figure 5(b).

Figure 6(a) shows the changes in the atomic percentages of W, F, and O on the W surface during one ALE cycle measured by XPS with the optimized W ALE conditions in Figure 4. For the reference sample, due to the surface oxidation of as-received W by environment, high oxygen percentage (probably W oxidation by air exposure) of $\sim 70.6\%$ was observed while $\sim 29.1\%$ of W and no fluorine were observed. After the adsorption with F radicals for 10 s, the F atomic

percentage was increased to $\sim 49.1\%$ similar to the saturated F atomic percentage shown in Figure 2(a) while decreasing atomic percentages of O and W. Through the removal of WF_y on the W surface by the O_x^+ ions for 3, 5, 8, and 10 s, the F atomic percentage was decreased to ~ 26.7 , ~ 21.3 , ~ 18 , and $\sim 10\%$ while increasing the atomic percentages of W and O. When the O_x^+ ion desorption time was further increased to 15 s, the atomic percentages of W, O, and F were remaining similar indicating no further removal of WF_y after 10 s of O_x^+ ion desorption time by exposing W metal itself.

Even though no change of F on W was observed in Figure 6(a) after 10 s of O_x^+ ion desorption time by exposing W metal itself, F atomic percentage of $\sim 10\%$ was remaining on the exposed W metal surface after one ALE cycle. To investigate the source of F remaining on the W metal surface after the W ALE, the Ar^+ ion depth profiling of W adsorbed with F radicals for 0–30 s during the adsorption step was conducted using XPS. The F atomic percentages in W with increasing Ar^+ ion depth profiling time of 0–60 s are shown in Figure 6(b). (The changes of atomic percentages of W and O with increasing the Ar^+ depth profiling time are shown in Figure S4). As the Ar^+ ion depth profiling condition, 10 mA and 2 kV of Ar^+ ion gun was used. After the F radical adsorption, the F atomic percentages were similar to those shown in Figure 2(a) and, with the increase of depth profiling time, F atomic percentages were continuously decreasing but not decreasing to zero percentage indicating the penetration of F atoms into W. However, F atomic percentage was significantly decreased after the first 10 s of depth profiling time to 10–15% of F and the further increase of depth profiling

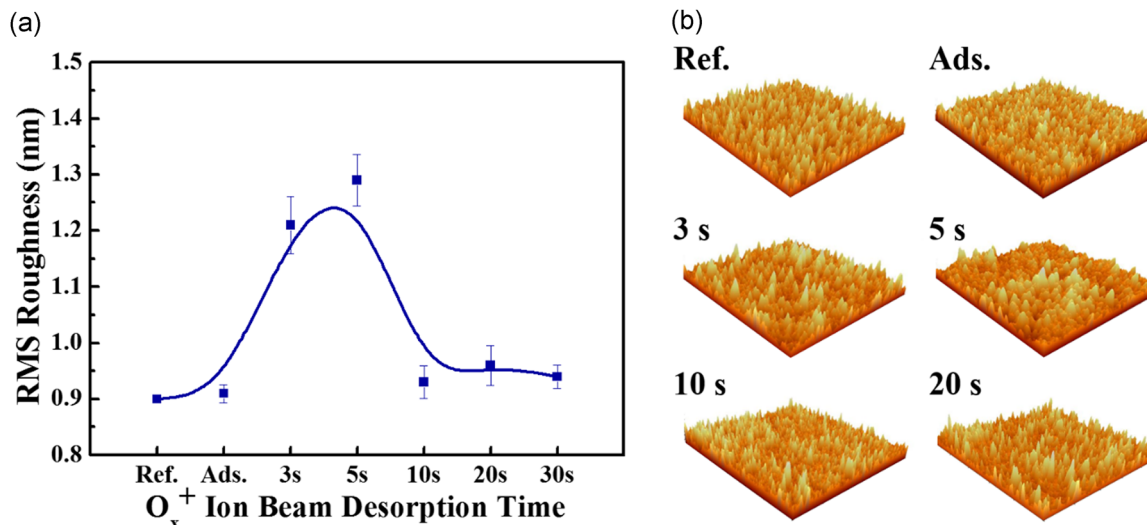


FIGURE 5 (a) Change of RMS surface roughness during one ALE cycle measured by AFM on $2.5\ \mu\text{m} \times 2.5\ \mu\text{m}$ W samples with the optimized W ALE condition. (b) AFM images for the conditions in (a). AFM, atomic force microscope; RMS, root mean square; W ALE, tungsten atomic layer etching

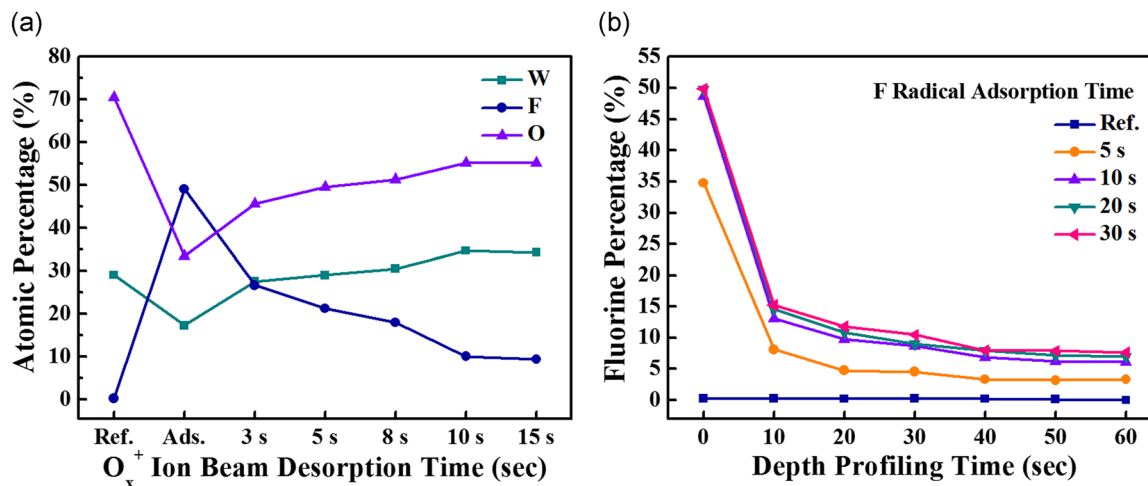


FIGURE 6 (a) Changes in the atomic percentages of W, F, and O on the W surface during one ALE cycle measured by XPS with the optimized W ALE conditions in Figure 4 (b) F atomic percentages measured on the W surfaces (F radical adsorbed for 5–30 s) by XPS as a function of depth profiling time. AFM, atomic force microscope; W ALE, tungsten atomic layer etching

time decreased the F atomic percentage slowly possibly indicating that most of F radicals were adsorbed on the W surface even though some F radicals were diffused into W. To remove the remaining F on the W surface after the W ALE cycle, heating after the ALE may be needed.

4 | CONCLUSION

Anisotropic ALE of W was investigated by sequentially exposing to F radicals by NF_3 plasma during the adsorption step and to an oxygen ion beam during the desorption step per etch cycle at room temperature for anisotropic and precise etching. During the adsorption step, F radicals were adsorbed on the W surface by forming WF_y compounds and, during the desorption step, the WF_y compounds on the W surface were removed by the formation of volatile WO_xF_y using the oxygen ion beam. Therefore, at the optimized W ALE conditions, a precise W etch rate of $\sim 2.6 \text{ \AA/cycle}$ could be obtained. A wide ALE window of F radical adsorption time of ($\geq 10 \text{ s/cycle}$ at 300 W ICP power) and O_x^+ ion desorption time of ($10 \leq t \leq 30 \text{ s/cycle}$ at 300 W ICP power and $+44 \sim 51 \text{ eV}$ of ion energy) could be identified even though the optimum F radical adsorption time and O_x^+ ion desorption time were 10 s each. At the optimized W ALE conditions, W etch depth was linearly increased with the number of etch cycles, the near infinite etch selectivity over SiO_2 was observed, and the surface roughness after the ALE was similar to the as-received W. However, after the W ALE, $\sim 10\%$ F diffused into W was observed on the W surface, and which could be removed by a following process such as an annealing process.

ACKNOWLEDGMENTS

This study was supported by the National Research Foundation of Korea (NRF) grant funded by the Korean government (MSIT) (2018R1A2A3074950) and the Nano Material Technology Development Program through the National Research Foundation Korea (NRF), funded by the Ministry of Education, Science, and Technology (2016M3A7B4910429).

ORCID

Geun Young Yeom  <http://orcid.org/0000-0002-1176-7448>

REFERENCES

- [1] C. T. Carver, J. J. Plombon, P. E. Romero, S. Suri, T. A. Tronic, R. B. Turkot, *ECS J. Solid State Sci. Technol* **2015**, *4*, N5005.
- [2] G. S. Oehrlein, D. Metzler, C. Li, *ECS J. Solid State Sci. Technol* **2015**, *4*, N5041.
- [3] K. J. Kanarik, S. Tan, R. A. Gottscho, *J. Phys. Chem. Lett.* **2018**, *9*, 4814.
- [4] K. J. Kanarik, T. Lill, E. A. Hudson, S. Sriraman, S. Tan, J. Marks, V. Vahedi, R. A. Gottscho, *J. Vac. Sci. Technol. A* **2015**, *33*, 020802.
- [5] A. Ranjan, M. Wang, S. D. Sherpa, V. Rastogi, A. Koshiishi, P. L. G. Ventzek, *J. Vac. Sci. Technol. A* **2016**, *34*, 031304.
- [6] D. Metzler, C. Li, S. Engelmann, R. L. Bruce, E. A. Joseph, G. S. Oehrlein, *J. Vac. Sci. Technol. A* **2016**, *34*, 01B101.
- [7] J. W. Park, D. S. Kim, M. K. Mun, W. O. Lee, K. S. KIM, G. Y. Yeom, *J. Phys. D Appl. Phys.* **2017**, *50*, 254007.
- [8] C. Kauppinen, S. A. Khan, J. Sundqvist, D. B. Suyatin, S. Suihkonen, E. I. Kauppinen, M. Sopanen, *J. Vac. Sci. Technol. A* **2017**, *35*, 060603.
- [9] J. W. Park, D. S. Kim, W. O. Lee, J. E. Kim, G. Y. Yeom, *Nanotechnol* **2019**, *30*, 085303.

- [10] W. S. Lim, Y. Y. Kim, H. Kim, S. Jang, N. Kwon, B. J. Park, J. H. Ahn, I. Chung, B. H. Hong, G. Y. Yeom, *Carbon* **2012**, *50*, 429.
- [11] K. S. Kim, K. H. Kim, Y. Nam, J. Jeon, S. Yim, E. Singh, J. Y. Lee, S. J. Lee, Y. S. Jung, G. Y. Yeom, D. W. Kim, *ACS Appl. Mater. Interfaces* **2017**, *9*, 11967.
- [12] S. S. Kaler, Q. Lou, V. M. Donnelly, D. J. Economou, *J. Phys. D Appl. Phys.* **2017**, *50*, 234001.
- [13] A. Agarwal, M. J. Kushner, *J. Vac. Sci. Technol. A* **2009**, *27*.
- [14] K. S. Kim, Y. J. Ji, Y. Nam, K. H. Kim, E. Singh, J. Y. Lee, G. Y. Yeom, *Sci. Rep* **2017**, *7*.
- [15] J. K. Kim, S. I. Cho, S. H. Lee, C. K. Kim, K. S. Min, S. H. Kang, G. Y. Yeom, *J. Vac. Sci. Technol. A* **2013**, *31*, 061310.
- [16] S. M. George, Y. Lee, *ACS Nano* **2016**, *10*, 4889.
- [17] Q. Jiang, M. Tsai, R. H. Havemann, *Proc. IEEE Int. Interconnect Technol. Conf.* **2001**, 227.
- [18] D. Choi, C. S. Kim, D. Naveh, S. Chung, A. P. Warren, N. T. Nuhfer, M. F. Toney, K. R. Coffey, K. Barmak, *Phys. Rev. B* **2012**, *86*, 045432.
- [19] D. Choi, B. Wang, S. Chung, X. Liu, A. Darbal, A. Wise, N. T. Nuhfer, K. Barmak, A. P. Warren, K. R. Coffey, M. F. Toney, *J. Vac. Sci. Technol. A* **2011**, *29*, 051512.
- [20] C. Fen chen, D. Gardner, *IEEE Electron Device Lett* **1998**, *19*, 508.
- [21] T. Sun, B. Yao, A. P. Warren, V. Kumar, S. Roberts, K. Barmak, K. R. Coffey, *J. Vac. Sci. Technol. A* **2008**, *26*, 605.
- [22] T. Sun, B. Yao, A. P. Warren, K. Barmak, M. F. Toney, R. E. Peale, K. R. Coffey, *Phys. Rev. B* **2009**, *79*, 041402.
- [23] T. Sun, B. Yao, A. P. Warren, K. Barmak, M. F. Toney, R. E. Peale, K. R. Coffey, *Phys. Rev. B* **2010**, *81*, 155454.
- [24] J. R. Lloyd, M. W. Lane, E. G. Liniger, C. K. Hu, T. M. Shaw, R. Rosenberg, *IEEE Trans. Device Mater. Reliab* **2005**, *5*, 113.
- [25] J. W. McPherson, in *Proc. Design Automation Conf.* **2006**, 176.
- [26] H. Shang, M. H. White, K. W. Guarini, P. Solomon, E. Cartier, F. R. McFeely, J. J. Yurkas, W. C. Lee, *Appl. Phys. Lett.* **2001**, *78*, 20.
- [27] B. D. Davidson, D. Seghete, S. M. George, V. M. Bright, *Sens. Act. A* **2011**, *166*, 269.
- [28] J. R. Lloyd, J. Clemens, R. Snede, *Microelectron. Reliab* **1999**, *39*, 1595.
- [29] C. S. Hau-Riege, *Microelectron. Reliab* **2004**, *44*, 195.
- [30] S. M. Rossnagel, T. S. Kuan, *J. Vac. Sci. Technol. B* **2004**, *22*, 240.
- [31] J. Tower, M. Gostein, K. Otsubo, A. Kawasaki, *Mat. Res. Soc. Symp. Proc.* **2003**, 766.
- [32] G. Wang, Q. Xu, T. Yang, J. Xiang, J. Xu, J. Gao, C. Li, J. Li, J. Yan, D. Chen, T. Ye, C. Zhao, J. Luo, *State Sci. Technol* **2014**, *3*, P82.
- [33] N. R. Johnson, S. M. George, *ACS Appl. Mater. Interfaces* **2017**, *9*, 34435.
- [34] W. Xie, P. C. Lemaire, G. N. Parsons, *ACS Appl. Mater. Interfaces* **2018**, *10*, 9147.

SUPPORTING INFORMATION

Additional supporting information may be found online in the Supporting Information section.

How to cite this article: Kim DS, Kim JE, Lee WO, et al. Anisotropic atomic layer etching of W using fluorine radicals/oxygen ion beam. *Plasma Process Polym.* 2019;e1900081.
<https://doi.org/10.1002/ppap.201900081>